A probabilistic analysis of human influence on recent record global mean temperature changes

CrossMark

Philip Kokic [a,b,*], Steven Crimp [c,1], Mark Howden [d,2]

[a] CSIRO, CCI, GPO Box 664, ACT 2601, Australia
[b] CSSM, University of Wollongong, Wollongong, NSW 2522, Australia
[c] CSIRO, CES, GPO Box 1700, ACT 2601, Australia
[d] CSIRO, CAF, GPO Box 1700, ACT 2601, Australia

A R T I C L E   I N F O

A B S T R A C T

December 2013 was the 346th consecutive month where global land and ocean average surface temperature exceeded the 20th century monthly average, with February 1985 the last time mean temperature fell below this value. Even given these and other extraordinary statistics, public acceptance of human induced climate change and confidence in the supporting science has declined since 2007. The degree of uncertainty as to whether observed climate changes are due to human activity or are part of natural systems fluctuations remains a major stumbling block to effective adaptation action and risk management. Previous approaches to attribute change include qualitative expert-assessment approaches such as used in IPCC reports and use of 'fingerprinting' methods based on global climate models. Here we develop an alternative approach which provides a rigorous probabilistic statistical assessment of the link between observed climate changes and human activities in a way that can inform formal climate risk assessment. We construct and validate a time series model of anomalous global temperatures to June 2010, using rates of greenhouse gas (GHG) emissions, as well as other causal factors including solar radiation, volcanic forcing and the El Niño Southern Oscillation. When the effect of GHGs is removed, bootstrap simulation of the model reveals that there is less than a one in one hundred thousand chance of observing an unbroken sequence of 304 months (our analysis extends to June 2010) with mean surface temperature exceeding the 20th century average. We also show that one would expect a far greater number of short periods of falling global temperatures (as observed since 1998) if climate change was not occurring. This approach to assessing probabilities of human influence on global temperature could be transferred to other climate variables and extremes allowing enhanced formal risk assessment of climate change.

Introduction

There is a clear upward trend in global temperatures from 1882 to 2013 with a number of short time periods of stable or falling temperatures (Fig. 1). Of particular note, from March 1985 to December 2013 there was an unbroken sequence of

---

* Corresponding author at: CSIRO, CCI, GPO Box 664, ACT 2601, Australia. Tel.: +61 2 6216 7043; fax: +61 2 6216 7111.
E-mail addresses: Philip.Kokic@csiro.au (P. Kokic), Steven.Crimp@csiro.au (S. Crimp), Mark.Howden@csiro.au (M. Howden).
[1] Tel.: +61 2 6246 4095.
[2] Tel.: +61 2 6246 4118.

average monthly temperatures exceeding the 20th century average for each corresponding month resulting in a total of 346 months. Such a fact would seem to strongly support the hypothesis that global warming is occurring, but the question remains: how strong is this evidence (Bowman et al., 2010)? Even given these and other extraordinary statistics as well as the body of evidence synthesised in the Intergovernmental Panel on Climate Change (IPCC, 2007, 2013) regarding climate trends, detection and attribution, public acceptance of human induced climate change and confidence in the supporting science has declined since 2007 (Leiserowitz et al., 2011). The degree of uncertainty as to whether observed climate changes are due to human activity or are part of natural systems fluctuations remains a major stumbling block to effective adaptation action and risk management. Consequently, there are calls for alternative analyses to better understand climate change risks as well as improved approaches to effectively communicate this risk (Bowman et al., 2010). Previous approaches to attribute change to human influence include qualitative expert-assessment approaches such as used in the IPCC reports and use of 'fingerprinting' methods based on global climate models. Here we develop an alternative approach which provides a rigorous statistical assessment of the link between observed climate changes and human activities in a way that can inform formal climate risk assessment.

The approach used here allows us to make probabilistic statements about the likelihood of this anomalous warming occurring in the presence or absence of anthropogenic GHG emissions. In this regard it complements and extends existing climate change detection and attribution research using dynamic global climate model simulations and optimal fingerprint analysis (Hegerl and Zwiers, 2011; Berliner et al., 2000; Allen et al., 2000; Hansen et al., 2010; Easterling and Wehner, 2009) and professional assessments of the literature (IPCC, 2007). For example, a value of 95% for the probability of anthropogenic climate change was given by the IPCC whereas our approach progresses research on the statistical detection of climate change (Hansen et al., 2010; Rhamstorf and Coumou, 2011) to include the probability of that change.

Recent research has begun to inspect this issue through attribution studies including examination of the effect of the global warming trend on temperate extremes and variability (Rhamstorf and Coumou, 2011; Medvigy and Beaulieu, 2012; Barriopedro et al., 2011; Hansen et al., 2012). Rhamstorf and Coumou (2011) suggest an approximate 80% probability that the July 2011 heat record in Moscow would not have occurred without global warming. Hansen et al. (2012) use a statistical summary analysis to illustrate changes in the distribution of the surface air temperature anomalies around the globe from 1951 to 2010, normalised by local standard deviation estimates. Their analysis indicated that both the location and spread of this distribution increased over time, but because no statistical model was constructed they were unable to test for the statistical significance of these changes.

Both the approaches of Rhamstorf and Coumou (2011) and Hansen et al. (2012) are limited in their ability to make firm probabilistic statements about the changes that are observed because neither uses a validated statistical model in their analysis. The statistically robust approach used in this paper, incorporates time series modelling, validation and bootstrap simulation and provides a probabilistic assessment of global warming, strongly complementing the scientific evidence for the anthropogenic origin of recent climate change. Methods that account for temporal dependencies in climate data have been considered before in the statistical downscaling literature; see e.g. Charles et al. (2004), but their emphasis was on model skill and projections rather than attribution, which is essential for the current application.

To construct the statistical model we use GHG concentration, solar radiation, volcanic activity and the El Niño Southern Oscillation cycle as these are key drivers of global temperature variance (IPCC, 2007, 2013; Meinshausen et al., 2011; Allan, 2000; Benestadt and Schmidt, 2009; Gohar and Shine, 2007; Wang et al., 2005). This analysis uses recorded data (NOAA National Climate Data Centre, 2011) avoiding the uncertainties that can arise in the complementary climate model-based fingerprint studies (Hegerl and Zwiers, 2011).

Observations of short periods where global mean temperatures have fallen, even though atmospheric concentrations of GHGs were rising, have also raised questions as to the causal link between concentrations and warming (Plimer, 2009). The
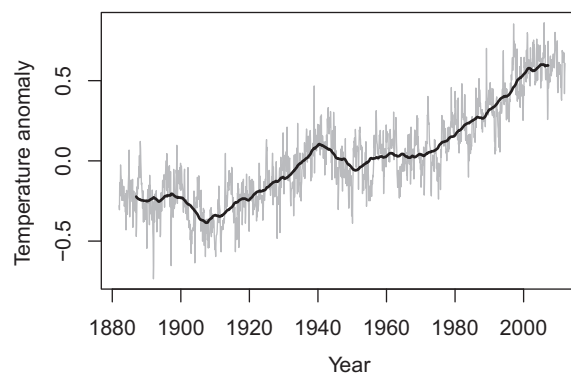
Fig. 1. Global monthly mean land and sea surface temperature anomaly: January 1882 to April 2012 time series relative to a 1901–2000 base period (grey line), and a 5 year running mean of this time series (black line) (*Source*: http://www.ncdc.noaa.gov/cmb-faq/anomalies.html). (Smith et al., 2008).

approach used in this paper is also used to determine the probability of events of declining temperatures with and without the effect of anthropogenic climate change.

Statistical approaches that detect and associate forcing effects using observations only have been criticised as they can assume the response to forcing is instantaneous or that climate change and variability can be separated by time (Hegerl and Zwiers, 2011). The time series model we use overcomes these issues, with evidence for how this is achieved presented in later sections of this paper.

Methodology and model fitting

Covariate data

There is strong physical evidence that the critical factors which influence global temperatures in the time-scale of human decision-making are atmospheric GHGs, aerosol and particulate concentrations, the El Niño Southern Oscillation (ENSO) cycle, solar radiation, and volcanic activity (IPCC, 2007, 2013; Meinshausen et al., 2011; Allan, 2000; Benestadt and Schmidt, 2009; Gohar and Shine, 2007; Wang et al., 2005). The covariate data used to represent these factors are as follows:

1. Equivalent carbon dioxide (eCO_2) – a combined measure of all major GHGs controlled under the Kyoto protocol calculated using carbon dioxide radiative forcing relationships integrated with the effects of aerosols and particulates (Gohar and Shine, 2007).
2. The Southern Oscillation Index (SOI) – a measure of ENSO variability measured by the pressure differences between Tahiti and Darwin (Allan, 2000).
3. Total solar irradiance – a measure of the incident sunlight received by the Earth's atmosphere (Benestadt and Schmidt, 2009); and
4. Volcanic stratospheric aerosol radiative forcing – a measure of the impact of volcanic activity (Meinshausen et al., 2011).

These covariate data (Fig. 2) were obtained from a variety of sources as presented in Table 1. Some of these data required post-processing to ensure consistency of record length and data frequency:

- SORCE TIM TSI (Wang et al., 2005) data was appended to the KNMI TSI (Benestadt and Schmidt, 2009) data from 2009 onwards by first aggregating it to monthly level, then adjusting it to the KNMI radiative forcing scale. The agreement between the two time series was extremely close (correlation = 0.99) during the overlapping time period.
- VOLRF data was only available up to, and including 2006. Besides the Eyjafjallajökull eruption in 2010, there was no volcanic activity which had a significant impact on global climate during the time period from January 2007 to June 2010 (Clarke et al., 2007; Meinshausen et al., 2011; Hegerl et al., 1977). Initial estimates of the effect of the Eyjafjallajökull eruption on global climate up to June 2010 were small (Meinshausen et al., 2011) therefore a mean value of zero for VOLRF was imputed during the time period from January 2007 to June 2010.
- Monthly values for VOLRF and eCO_2 were obtained by linear interpolation from the annual time series. Thus seasonal variation is not present in these time series but this will be accounted for in the statistical model.
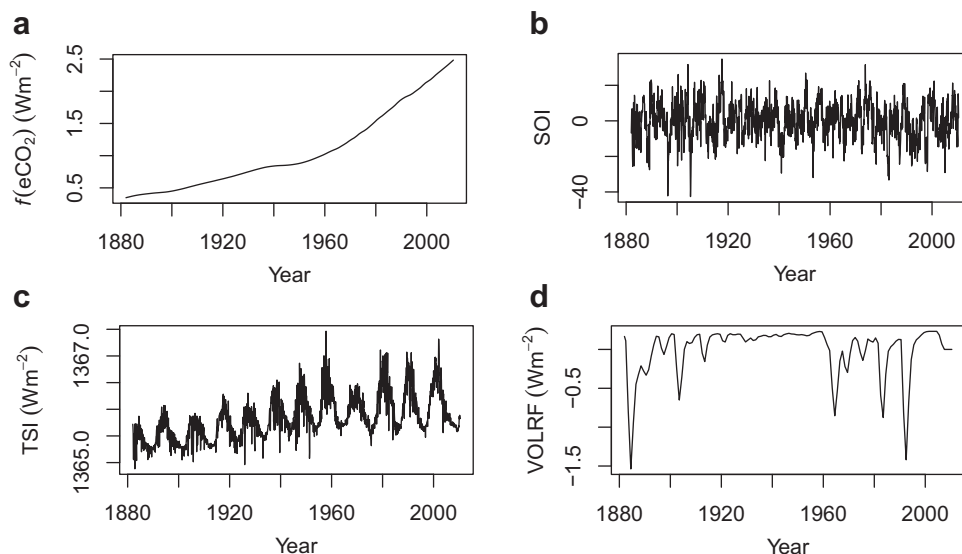

Fig. 2. Time series plots of the data used for statistical modelling.

Table 1
Covariate data used for statistical modelling of global mean temperature anomalies.

Time series	Forcing	Source	Time period	Frequency
eCO$_2$ (Clarke et al., 2007)	Major GHGs	RCP database (version 2) http://www.iiasa.ac.at/web-apps/tnt/RcpDb	1765–2010	Annual (mid –year)
SOI	ENSO	Australian Bureau of Meteorology: ftp://ftp.bom.gov.au/anon/home/ncc/www/sco/ soi/soiplaintext.html	1876–2010	Monthly
TSI (Wang et al., 2005)	Solar irradiance	KNMI Climate explorer http://climexp.knmi.nl/getindices.cgi?FUBData/ tsi_wls_mon+reconstructed_solar_constant+ i+someone@somewhere	1882–2008	Monthly
		SORCE TIM TSI http://lasp.colorado.edu/sorce/data/tsi_data.htm	2003–2010	Daily
VOLRF (Meinshausen et al., 2011)	Volcanic stratospheric aerosol	RCP database (version 2) http://www.iiasa.ac.at/web-apps/tnt/RcpDb	1765–2006	Annual

To conform to the approximate physical relationship between greenhouse gas concentration and temperature, eCO$_2$ was converted to a radiative forcing value using the approximation $f(eCO_2) = 5.35 \log_e(eCO_2/278)$ (Myhre et al., 1998). These relationships also imply that temperature (in a closed system) increases linearly with the radiative forcing value of an input, suggesting that a multiple linear regression is a suitable approximation for modelling the global mean temperature anomaly. We examine the evidence for linearity in greater detail below. The correlations between the covariates are mostly small (Fig. 3), and if they are recomputed over the period January 1950 to June 2010 when global mean temperature rises more dramatically, the 0.48 correlation between eCO$_2$ and TSI reduces to 0.04. Thus one may interpret the magnitude of each regression coefficient as being mostly due to the effect of the variable to which it is associated. This issue is also explored further below. Finally, due to the fact that certain minor causal variables may have been omitted, and also because the monthly series of eCO$_2$ and VOLRF were interpolated from the annual time series, it is likely that the residuals from such a regression model are serially correlated. Given this analysis is based on contemporary temperature records contingent with rapid human-caused perturbations of GHG emissions, it is likely that our analysis is only considering the causal effect of the growing emissions on mean global temperature and not the positive feedbacks known to occur over longer time-scales (IPCC, 2007, 2013).

The time series regression model

Let y_t, $t = 1, \ldots, T$, be the mean global temperature anomaly in month t, where $t = 1$ corresponds to January 1882 and $T = 1542$ corresponds to June 2010. Let $x_{1t}, \ldots, x_{4t}$ be the values of the four covariates; $f(eCO_2)$, SOI, TSI and VOLRF, respectively, at time t. As described above, a time series regression model of the form:

$$y_t = \mu + \sum_{j=1}^{4} \beta_j x_{jt} + \eta_t \tag{1}$$

was fitted to the data, where η_t has an ARMA structure (Shumway and Stoffer, 2011). The arima function in R (http://www.r-project.org/) can be used to fit a regression model of the form (1). This model was used as it can accurately represent residual autocorrelation in regression, and hence can provide a realistic stochastic representation of a time series suitable for simulation, as well as an unbiased assessment of the statistical significance of regression coefficients compared to those obtained from ordinary least squares regression (Maddala, 2001).

The model was selected according to a Bayesian Information Criterion (BIC) using the auto.arima function in R (Hyndman and Khandakar, 2008) with default parameters and a search restricted to stationary models, and the entire time series from 1882 to 2010 was used. We start with the simple (stationary in this case) and only move to the complex (non-stationary) if the performance of the simpler model was found to be wanting. The selected model has autoregressive terms of order 1, and moving average terms of orders 1 and 2 (Table 2, Model A). However, the partial autocorrelation plot indicated strong autocorrelation for a lag of 24 months. Therefore, moving average terms of lags 12 and 24, were added to the model (Table 2, Model B). The residual for this model is of the form:

$$\eta_t = \varepsilon_t + \theta_1 \varepsilon_{t-1} + \theta_2 \varepsilon_{t-2} + \theta_{12} \varepsilon_{t-12} + \theta_{24} \varepsilon_{t-24} + \varphi_1 \eta_{t-1}, \tag{2}$$

where ε_t are independent identically distributed random variables with mean zero and variance σ^2, and ϕ_1 and $\theta_1, \theta_2, \theta_{12}, \theta_{24}$, are unknown constants. The lag 1 and 2 terms in this model capture short-term dependencies in the monthly global temperature time series, while the lag 12 and 24 terms account for longer-term dependencies. The diagnostics for this model are very good and will be described in greater detail in Section "Model diagnostics" below. Model B was also refitted to the HadCRUT3 temperature anomaly data (http://www.cru.uea.ac.uk/cru/data/temperature/) constructed by the UK Meteorological Office and the Hadley Centre (Table 2, Model C). It can be clearly seen from the table that the parameter estimates

Table 2

Parameter estimates of the time series regression models. Values in parentheses are standard errors of the parameter estimates. See the text for an explanation.

Model		A	B	C	D	E
Data		NCDC		HadCRUT3	NCDC	
Time period for fitting		1882–2010				1950–2010
Regression parameter (β)	$f(eCO_2)$	0.38 (0.03)**	0.38 (0.03)**	0.40 (0.03)**	0.38 (0.03)**	0.42 (0.03)**
	SOI	−0.0013 (0.0004)**	−0.0013 (0.0004)**	−0.0012 (0.0003)**	−0.0012 (0.0004)**	−0.0012 (0.0003)**
	TSI	0.008 (0.012)	0.007 (0.012)	0.007 (0.013)	0.008 (0.012)	−0.008 (0.015)
	VOLRF	0.09 (0.04)*	0.09 (0.04)*	0.10 (0.05)*	0.09 (0.04)*	0.10 (0.04)*
Autoregressive parameter	ϕ_1	0.93 (0.01)**	0.93 (0.01)**	0.91 (0.02)**	0.92 (0.02)**	0.85 (0.02)**
	ϕ_2					
	ϕ_{12}				0.13 (0.18)	
	ϕ_{24}				0.56 (0.17)**	
Moving average parameter	θ_1	−0.45 (0.03)**	−0.44 (0.03)**	−0.41 (0.03)**	−0.44 (0.03)**	−0.35 (0.05)**
	θ_2	−0.08 (0.03)**	−0.08 (0.03)**	−0.03 (0.03)	−0.07 (0.03)**	−0.04 (0.05)**
	θ_{12}		0.01 (0.03)	0.03 (0.03)	−0.11 (0.19)	−0.01(0.04)
	θ_{24}		0.09 (0.02)**	0.08 (0.02)**	−0.47 (0.17)**	−0.06 (0.04)
BIC		−2880.5	−2879.6	−2686.3	−2872.3	−1402.4
AIC		−2928.6	−2938.4	−2745.1	−2941.7	−1452.8

* Statistically significant at the 5 percent level.
** Statistically significant at the 1 percent level.

for both time series are very similar, which gives us further confidence that the model is appropriate for these data. We also used the Akaike Information Criteria (AIC) and this resulted in a slightly more complicated model involving autoregressive terms of orders 1, 2, 12 and 24, and moving average terms of the same orders (Table 2, Model D). The regression parameters are again very similar to Model B, but there is only a minor improvement in AIC, indicating that the more parsimonious Model B is preferable. Finally, to test the stability of the parameter estimates, Model B was refitted to the time series from 1950 onwards (Table 2, Model E). Again most parameters changed by only a small amount and are within the 95% confidence intervals of the Model B parameters. The only exception to this is the autoregressive order 1 parameter which has reduced in magnitude slightly. The reason for this is unclear, but it may reflect an improvement in the data quality over time. For this reason we consider both Models B and E in the simulation study (see Table 2).

For the NCDC data, the analysis revealed that greenhouse gases (eCO₂) are the main contributing factor to the increase in global mean temperature since 1882 (Fig. 6a), which is consistent with the findings from other studies (IPCC, 2007, 2013; Allen et al., 2000; Hansen et al., 2010). The regression coefficient for $f(eCO_2)$ was estimated to be 0.38. This implies that from 1882 to 2010, for an increase of 100 ppm of eCO₂ the global mean temperature has increased on average by approximately 0.59 °C, which is similar to findings from dynamic climate models (Tett et al., 1999; Hegerl et al., 1977; Hegerl and Zwiers, 2011). The corresponding estimates for SOI was −0.0013, and for the TSI and VOLRF coefficient estimates were 0.007 and 0.09, respectively. Note the coefficient estimate for TSI is statistically insignificant, consistent with prior findings, where solar irradiation was found to be a minor contributor to global warming (Allen et al., 2000).

Exploring non-linearity and approximate orthogonality of covariates

As already noted above, for theoretical reasons we may expect a linear relationship between the radiative forcing covariates and global mean temperature. To explore this issue in greater detail we fitted non-parametric curves, as recommended by Fox and Weisberg (2011), to the scatter plots of each covariate against the mean global temperature anomaly (Fig. 4). These figures showed only a slight degree of non-linearity. However, they do not account for dependencies in the data, and so we refitted Model A using the gamm function from the mgcv library in R. We specified the same residual autocorrelation structure when fitting this model, but instead of linear functions we used non-parametric splines for all 4 covariates. Note that it is not possible to fit the other models with the gamm function because of their complicated autocorrelation structure, but this should only have minor influence on the curvature of the splines. The four splines were estimated to be exactly linear and coincided very closely to the arima function estimates (Fig. 4). Hence, it was concluded that a multiple linear regression was an accurate representation for modelling the mean global temperature anomaly.

Also, as already noted, the correlation between the covariates is very small for the data from 1950 onwards, thus one would not expect collinearity to be an issue. To examine whether this is indeed the case, each covariate was removed from Model B, one at a time, and the remaining parameters were re-estimated. In all cases the regression parameters only changed by a small amount. For example, when $f(eCO_2)$ was removed, the new regression parameter estimates for SOI, TSI and VOLRF were −0.013, 0.008 and 0.10, respectively, all within the 95% confidence intervals of the original estimates. Also note that the regression parameter estimates for Model E, fitted with data from 1950 onwards, are very similar to Model B. Thus we can safely interpret the regression coefficient as mostly representing the effect of the variable they are associated with.
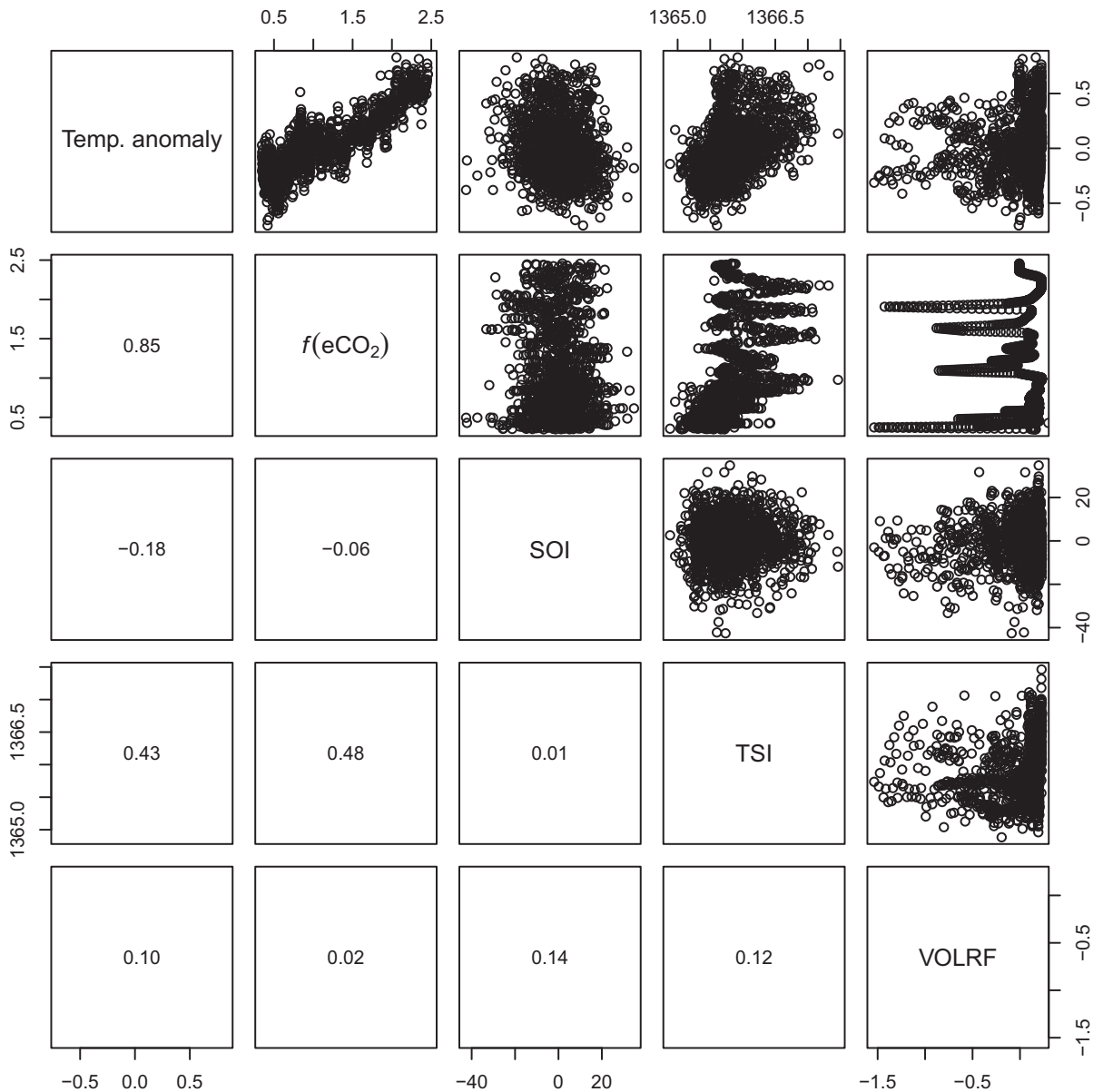
Fig. 3. A pairwise scatter plot matrix of the four covariates and the dependent variable. Variable names are indicated on the diagonal panels and Pearson correlation coefficients are given in the lower left-hand panels.

Lagged effects, feedback and other effects

When GHG concentrations vary, the radiative imbalance that is created can persist for a period of time as the system adjusts. Thus there may be lagged effects from the forcing factors. However, due to the approximate exponential shape of $f(eCO_2)$, lagged effects from this term are already effectively incorporated in the model. This follows because the sum of lagged terms of an exponentially shaped covariate is proportional to the same non-lagged covariate. Also, cross autocorrelation plots between each forcing term and the innovation residuals strongly indicate that lagged effects are accounted for by the model (Fig. 5d).

Multiple bootstrap simulations of global temperature were generated using the same observed history of the four forcing factors (Section "Model diagnostics"). The reason that this approach is valid is because there is virtually no feedback of mean global temperature to any of the forcing factors. In Power and Smith (2007), evidence was presented indicating that global warming may have slightly decreased the mean level of SOI from 1977 onwards, but no evidence was found indicating that it had affected the variation around the mean. This minor feedback effect can be removed by first subtracting a 30-year
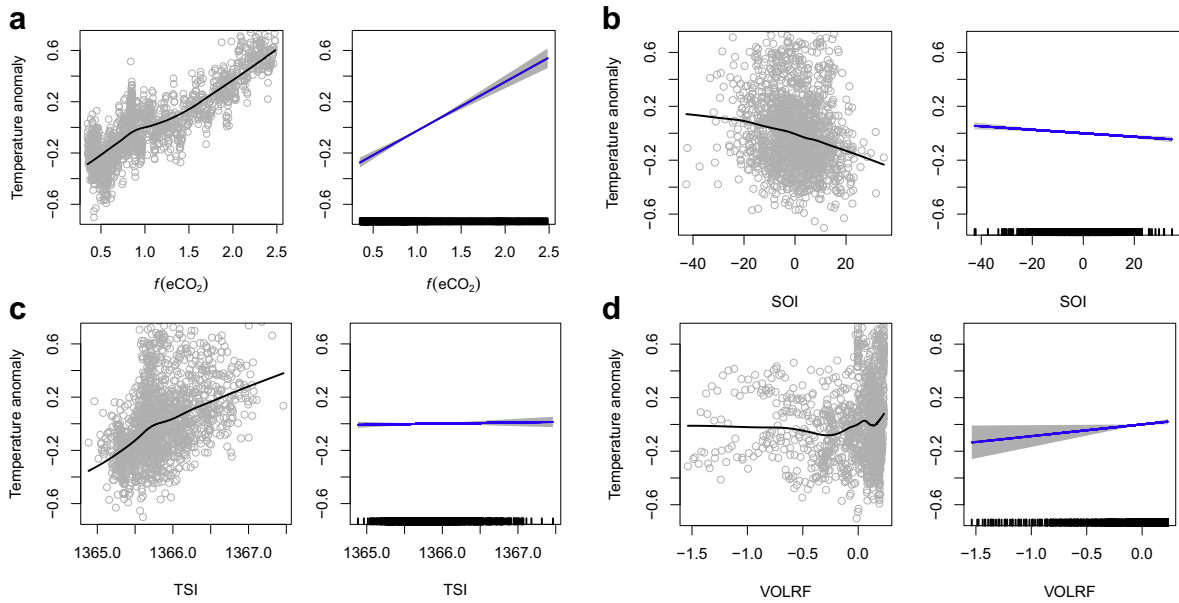
Fig. 4. Scatter plots and non-linear smooths of mean global temperature anomaly against the four covariates (left-hand figures in a–d). The lowess function in R (http://www.r-project.org/) with default parameters was used to smooth these data. The right hand figures in a–d are the fitted spline curves from the gamm function in R using the same autocorrelation structure as Model A.

running mean from the SOI time series (Power and Smith, 2007). When this was done and the time series Model B refitted almost identical parameter estimates were obtained to those shown in Table 2. For example, the coefficient estimate for SOI was identical to four decimal places.

Inclusion of variables representing both the Pacific Decadal Oscillation (PDO) and Quasi Biennial Oscillation (QBO) were also tested. These were found to be statistically significant but both had very minor impact on overall model fit. Because the PDO index is confounded with global temperatures, and the QBO index is only available from 1953 onwards, both these variables were subsequently excluded from the statistical model.
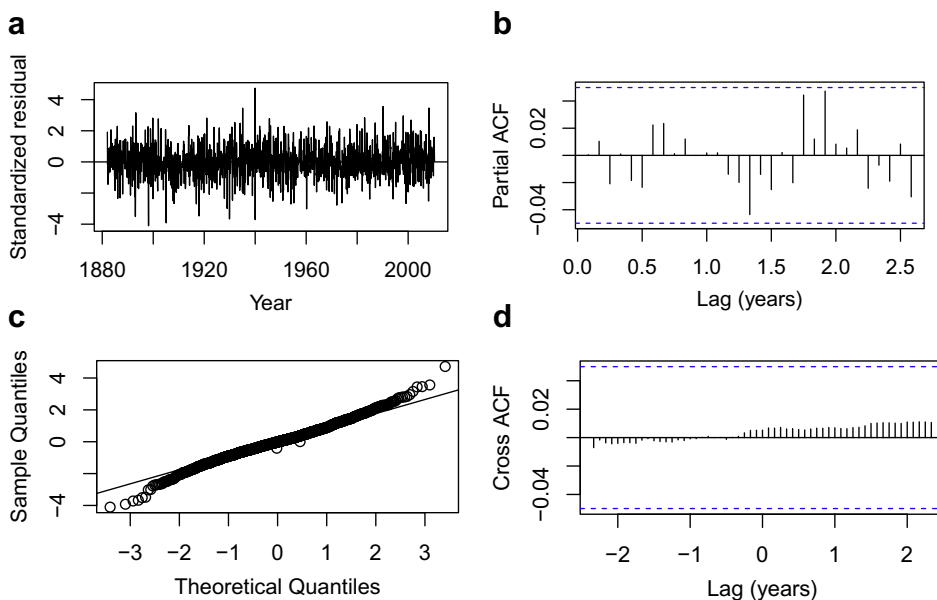
Fig. 5. Model diagnostic plots: (a) standardized innovation residuals against time. (b) Partial autocorrelation plot of the residuals. (c) Quantile–quantile plot of the standardized residuals. (d) Cross autocorrelation plot between the residuals and $f(eCO_2)$.

Model diagnostics

Fig. 5 presents various standard time series diagnostic plots of the model fitted to the NCDC temperature anomaly data. Fig. 5a illustrates that the standardized innovation residuals appear to be random with no evident outliers and constant variance. The partial autocorrelation plot (Fig. 5b) strongly indicates that the main autocorrelations of the model residuals have been adequately represented by expression (2). Furthermore, the Ljung-Box test (Ljung and Box, 1978) supports the hypothesis that all autocorrelations of the residuals up to lag 24 are zero (*p*-value = 0.26). The Breusch–Pagan test (Maddala, 2001) was non-significant further supporting the hypothesis that the residuals are homoscedastic. However, a Q-Q plot of the standardized innovation residuals (Fig. 5c) suggests that the tails of the residual distribution are slightly heavier than that of a normal distribution. In addition, the Shapiro–Wilk test (Royston, 1982) yields a *p*-value of less than 0.01 which also indicates that the residuals are non-normal. These facts together support the need to use a non-parametric bootstrap when simulating the global temperature anomaly time series even though little difference was observed in the simulation results between this and when the parametric bootstrap was used. Mild departures from the validated modelling assumptions examined in this section may occur for a variety of reasons (Brohan et al., 2006), but the simulation results presented below indicate that, even if they exist, they have only had a minor impact.

Bootstrap simulation

Bootstrap simulation (Efron and Tibshirani, 1994; Shumway and Stoffer, 2011) of the residual time series was performed using the arima.sim procedure in R and by randomly re-sampling the innovation residuals. Using the current parameter estimates, the covariate terms were then added to the simulated residuals via expression (1) to generate a single bootstrap sample of the original temperature anomaly time series. Each of the monthly simulated series had to also be mean-adjusted to ensure that, like the original series, their 20th century average was zero. To realistically represent uncertainty in the parameter estimates a double bootstrapping procedure was performed. The first bootstrap sample was used to simulate the parameter estimates, and the second bootstrap was used to simulate the time series using the first bootstrap parameter estimates. The various climate statistics were then calculated, e.g. the length of the longest sequence with mean monthly temperature exceeding the 20th century average of the corresponding month. By repeating the bootstrap simulation procedure a large number of times the distribution of such statistics was estimated.

Excluding eCO_2 from the simulations

To simulate what would have happened if the global temperature was not affected by rising levels of GHGs, the regression coefficient corresponding to eCO_2 in equation (1) was set to zero and the bootstrap simulation procedure followed.

One question asked when developing the statistical model was "Can the data be used to justify setting the eCO_2 coefficient to zero to represent a world not affected by climate change?". During the time period up to 1950 $f(eCO_2)$ didn't increase as rapidly as in more recent decades (Fig. 2a), but it's proportional contribution is unlikely to have changed, as will be shown in subsequent analysis. So it is reasonable to fit Model B to the time series up to 1950, but with GHGs excluded (that is without the x_{1t} term). The parameter estimates are within error bounds of the corresponding estimates for the model including eCO_2 fitted to the entire time series, but with the eCO_2 coefficient set to zero (Table 3). Furthermore, when simulations are reproduced using the estimates from Table 3, very similar results are obtained (Section "Simulation results"). These facts together provide empirical justification that setting the eCO_2 coefficient to zero in Model B represents global temperatures largely unaffected by climate change.

Multiple iterations (i.e. 100,000) of global temperature were generated using the same observed history of the four forcing factors resulting in stochastic alternatives to the way the global mean temperature anomaly may have evolved since the late 19th Century. A single simulation of the time series is illustrated in Fig. 6b with the effect of eCO_2 (black) and without its effect (blue). Specifically, the latter was produced by setting the eCO_2 forcing coefficient to zero. It can be seen that the simulated series including the effect of eCO_2 provides a good representation of the observed time series (Fig. 1), and major departure of the two simulated series occurs around 1960, which is consistent with analysis presented in the IPCC Fourth Assessment Report from dynamic climate models (IPCC, 2007). If questions about the effect of eCO_2 on global temperatures (Plimer, 2009) are valid then one should entirely exclude eCO_2 from the time series modelling. When this is implemented, an inaccurate representation of historical global temperature change results (Fig. 6c). The reason for this is that the estimated model in this case is close to non-stationary and so it behaves much like a random walk.

Simulation results

By June 2010 (the last date of the full data set available at the time of submission), regardless of which of the two global temperature series is examined, there are 304 consecutive months where global land and ocean average surface temperature exceeded the 20th century average for the corresponding month (NOAA National Climate Data Centre, 2011). To determine the probability of this happening with either eCO_2 forcing included or excluded, one hundred thousand bootstrap simulations of the temperature time series from the time series model were produced. The length of the longest sequence of

Table 3

Parameter estimates of the time series regression model using the NCDC global mean temperature anomaly time series including and excluding the effect of eCO_2. Note that data up to January 1950 was used to fit the model excluding eCO_2, whereas the entire time series was used to fit the model including eCO_2. Values in brackets are standard errors of the parameter estimates.

Model		B	F
	Covariate	Including eCO_2	Excluding eCO_2
Time period for fitting		1882–2010	1882–1949
Regression parameter (β)	$f(eCO_2)$	0.38 (0.03)[**]	
	SOI	−0.0013 (0.0004)[**]	−0.0012 (0.0004)[**]
	TSI	0.007 (0.012)	0.022 (0.018)
	VOLRF	0.09 (0.04)[*]	0.14 (0.07)[*]
Time series parameters	ϕ_1	0.93 (0.01)[**]	0.97 (0.01)[**]
	θ_1	−0.44 (0.03)[**]	−0.49 (0.04)
	θ_2	−0.08 (0.03)[**]	−0.15 (0.04)[**]
	θ_{12}	0.01 (0.03)	0.03 (0.04)
	θ_{24}	0.09 (0.02)[**]	0.11 (0.03)[**]

[*] Statistically significant at the 5 percent level.
[**] Statistically significant at the 1 percent level.
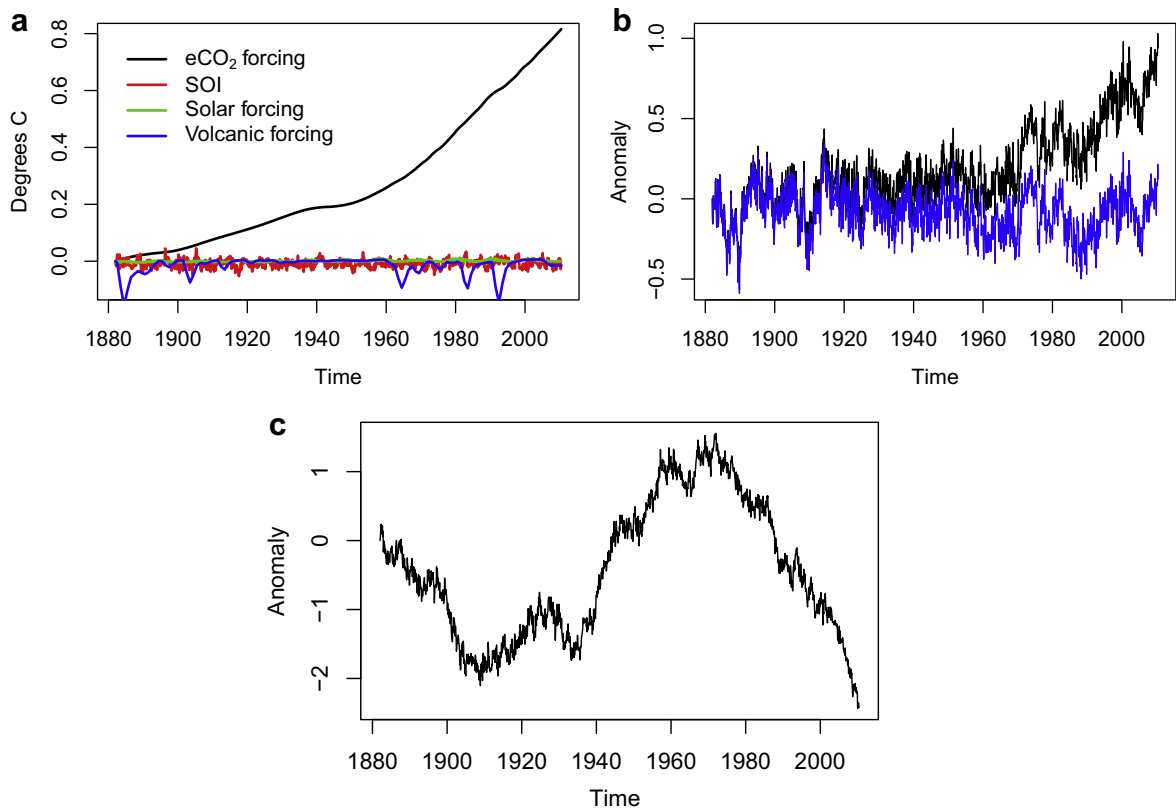
Fig. 6. Modelling results: (a) Estimated contribution of forcings to global mean temperature anomaly relative to January 1882 derived from the time series regression analysis. (b) Example simulation of global mean temperature anomaly with the effect of eCO_2 (black) and without the effect of eCO_2 (blue). (c) Example simulation of global mean temperature when eCO_2 forcing has been excluded from the model. To facilitate easy comparison the time series in these figures have been shifted so they start at zero in January 1882.

consecutive months between January 1950 and June 2010 with temperature exceeding the 20th century average was calculated. Fig. 7a shows boxplots of these simulated values for Models B, E and F. The chance of observing 304 consecutive months or more with temperature exceeding the 20th century average for the corresponding month is approximately 24.9 percent when eCO_2 forcing is included in Model B and 52.9 percent in Model E (Fig. 7a). When eCO_2 forcing is excluded from the simulations the probability of this occurring is less than 0.001 percent for both Models B and E. Under the scenario
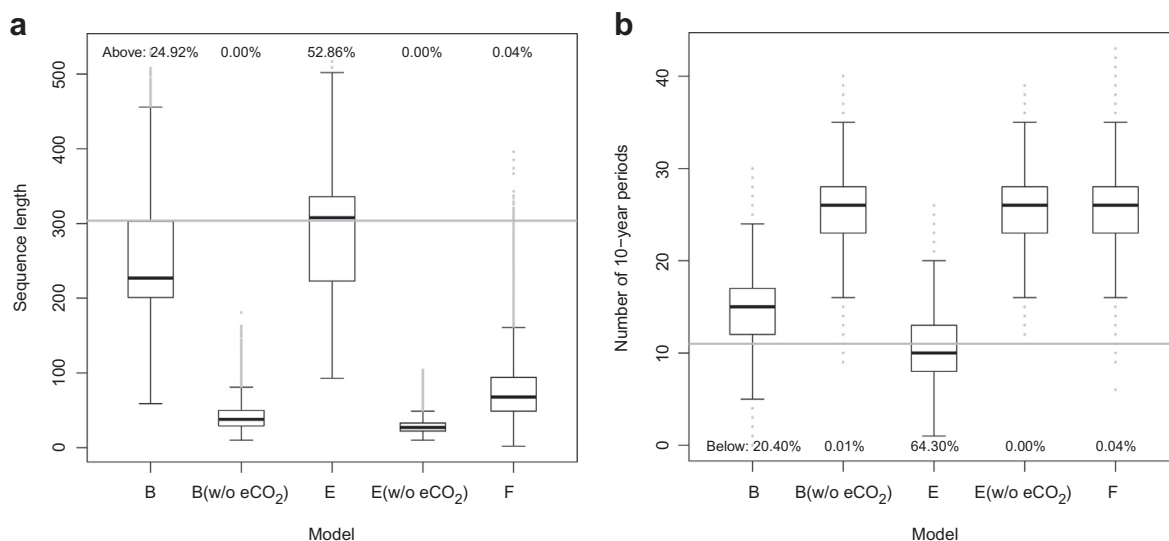
Fig. 7. Results from 100,000 bootstrap simulations of the global mean temperature anomaly time series from the time series regression model. (a) The distribution of the length of the longest sequence of global monthly average temperatures during the time window from January 1950 to June 2010 above the 20th century mean of the corresponding month. The grey line is the length of the longest sequence from the observed data. (b) Distribution of the number of non-increasing 10-year periods between January 1950 to June 2010 (i.e. with negative ordinary least squares regression coefficients for any given 10-year period). The grey line is the number of non-increasing 10-year periods from the observed data. Percentages of simulated values above or below the grey line are given.

that climate like that observed from 1882 to 1949 had continued to 2010 (Model F, Table 3), the chance of observing the anomalous temperature event is also very small; only about 0.04 percent. This result lends very strong support to the conclusion that such an anomalous climate event would not have occurred without the GHG emissions over recent decades. The observed value of 304 months is a single outcome of a real process, and the statistical models including the eCO_2 forcing, which is an accurate stochastic representation of the process, is consistent with this outcome in the sense that a single simulated value close to the observed value would not be unexpected, whereas for the models excluding eCO_2 such an outcome would be extremely unlikely (Fig. 7a).

Observations of short periods where global mean temperatures have fallen, even though atmospheric concentrations of GHGs have increased has raised questions as to the causal link between concentrations and warming (Plimer, 2009). A typical way this can be determined is to check for a non-positive coefficient for the ordinary least squares regression of global mean temperature against time for each 10-year period. For consistency with the previous analysis we used the same time window as above from January 1950 during which GHGs have been consistently rising. There were 11 such (potentially overlapping) time periods with falling temperatures between 1950 and 2010 (Fig. 1). The same bootstrap simulation described above was performed including and excluding eCO_2 forcing (Fig. 7b). When eCO_2 forcing is included in the analysis, a median of 15 periods of apparent falling decadal temperatures would be expected according to Model B and 10 periods according to Model E, and thus the 11 observed since 1950 are not unexpected. In fact, 11 is approximately the 20th percentile of the simulated values from Model B in this case. However, when eCO_2 is excluded from the analysis and so does *not* influence global mean temperature, a median of 26 such periods are simulated from Model B. In fact, none of the 100,000 simulations from Model E (excluding eCO_2) in this instance produced 11 or fewer decadal periods of falling temperatures. For Model F only 0.04 percent of the simulations produced 11 or fewer decadal periods of falling temperatures.

It is also interesting to examine the combined anomalous event of 11 or fewer decadal periods of falling temperature *and* 304 consecutive months where global land and ocean average surface temperature exceeded the 20th century average. This event was not observed in any of the 100,000 simulations of Model F, while it was observed in 37 percent of the simulations of Model E.

Discussion

The stochastic modelling exercise described above is the first demonstration of an extremely high probability for the link between GHGs and global warming using defensible statistical modelling techniques and observational data. In this regard it complements and extends existing climate change detection and attribution research using dynamic global climate model simulations and optimal fingerprint analysis (Hegerl et al., 1977; Berliner et al., 2000; Allen et al., 2000; Hansen et al., 2010; Easterling and Wehner, 2009) and professional assessments of the literature (IPCC, 2007).

The results of our statistical analysis would suggest that it is highly likely (99.999 percent) that the 304 consecutive months of anomalously warm global temperatures to June 2010 is directly attributable to the accumulation of global greenhouse gases in the atmosphere. The corollary is that it is extremely unlikely (0.001 percent) that the observed anomalous warming is not associated with anthropogenic GHG emissions. Solar radiation was found to be an insignificant contributor to global warming over the last century, which is consistent with the earlier findings of Allen et al. (2000).

During the period January 1950 to June 2010 there were 11 periods when global 10-year temperatures declined. Our study shows that in the absence of global warming an average of 25 such periods could have been expected. There is only a 0.01 percent chance of observing the recorded 11 events (or fewer) in the absence of recent global warming. Even when GHG emissions are included, the observed number of cooling periods is low compared with an average of 15 events simulated. Thus, rather than being an indicator that global warming is not occurring (Plimer, 2009), the observed number of cooling periods reinforces the case in support of recent global warming due to human influence. Furthermore it was found that the occurrence of either these cooling events or the anomalous record temperature event is highly improbable if climate similar to that between 1882 and 1949 had continued through to 2010. This result lends very strong supports to the conclusion that such anomalous climate events would not have occurred without the GHG emissions and climate change of recent decades.

Climate risk management covers a broad range of potential actions, including: early-response systems, strategic diversification, dynamic resource-allocation rules, financial instruments, infrastructure design and capacity building (Osgood and Hellmuth, 2009). In addition to avoiding adverse outcomes, climate risk management seeks to maximize opportunities in climate-sensitive economic sectors through improved resource management. Underpinning these activities is the provision of robust information regarding the return periods and probabilities of extremes. The degree of uncertainty as to whether observed climate changes are due to human activity or are part of natural systems fluctuations remains a major stumbling block to effective adaptation action and climate risk management. Through this analysis we hope that by reducing the uncertainty relating to the link between recent anomalous climatic events and global climate change and by demonstration of the capacity to provide rigorous probabilistic assessment that climate change information will be more readily included in risk management planning.

"A balanced portfolio of prospective, corrective and compensatory risk management strategies is the most cost-effective way to reduce disaster risks and support development." (Global Assessment Report on Disaster Risk Reduction, 2011). The current paper clearly informs this balance as it establishes the stochastic features and significance of causal factors that determine climate risk, and hence provide information that would underpin the prospective and corrective elements of risk management. Without this understanding there is a greater degree of incomplete information about the risks being faced which has the potential to render risk management strategies ineffective.

A major contributor to this inefficiency, in terms of limited uptake is the perceived controversy (Leiserowitz et al., 2011) of incomplete information used for climate risk management, and the consequent speculation about attribution of the causes of observed change (e.g. Plimer, 2009), which the current paper addresses effectively.

Acknowledgments

References

Allan, R.J., 2000. ENSO and climatic variability in the past 150 years. In: Diaz, H.F., Markgraf, V. (Eds.), ENSO: Multiscale Variability and Global and Regional Impacts. Cambridge University Press, Cambridge, pp. 3–55.

Allen, M.R., Stott, P.A., Mitchell, J.F.B., Schnur, R., Delworth, T.L., 2000. Quantifying the uncertainty in forecasts of anthropogenic climate change. Nature 407, 617–620.

Barriopedro, D., Fischer, E.M., Luterbacher, J., Trigo, R.M., García-Herrera, R., 2011. The hot summer of 2010: redrawing the temperature record map of Europe. Science 332, 220–224. http://dx.doi.org/10.1126/science.1201224.

Benestadt, R.E., Schmidt, G.A., 2009. Solar trends and global warming. J. Geophys. Res. 114, 1–18.

Berliner, L.M., Levine, R.A., Shea, D.J., 2000. Bayesian climate change assessment. Am. Meteorol. Soc. 13, 3805–3820.

Bowman, T.E., Maibach, E., Mann, M.E., Somerville, R.C.J., Seltser, B.J., Fischhoff, B., Gardiner, S.M., Gould, R.J., Leiserowitz, A., Yohe, G., 2010. Time to take action on climate communication. Science 330, 1044. http://dx.doi.org/10.1126/science.330.6007.1044.

Brohan, P., Kennedy, J.J., Harris, I., Tett, S.F.B., Jones, P.D., 2006. Uncertainty estimates in regional and global observed temperature changes: a new data set from 1850. J. Geophys. Res. 111, D12106.

Charles, S.P., Bates, B.C., Smith, I.N., Hughes, J.P., 2004. Statistical downscaling of daily precipitation from observed and modelled atmospheric fields. Hydrol. Process. 18, 1373–1394.

Clarke, L., Edmonds, J., Jacoby, H., Pitcher, H., Reilly, J., Richels, R., 2007. Scenarios of Greenhouse Gas Emissions and Atmospheric Concentrations. Sub-report 2.1A of Synthesis and Assessment Product 2.1 by the U.S. Climate Change Science Program and the Subcommittee on Global Change Research. Department of Energy, Office of Biological & Environmental Research, Washington, DC, USA. p. 154.

Easterling, D.R., Wehner, M.F., 2009. Is the climate warming or cooling? Geophys. Res. Lett. 36, L08706. http://dx.doi.org/10.1029/2009GL037810.

Efron, B., Tibshirani, R., 1994. An Introduction to the Bootstrap. Chapman & Hall/CRC.

Fox, J., Weisberg, S., 2011. An R Companion to Applied Regression, second ed. SAGE Publications.

Global Assessment Report on Disaster Risk Reduction, 2011. Revealing Risk, Redefining Development. UNISDR, Geneva, Switzerland.

Gohar, L.K., Shine, K.P., 2007. Equivalent CO_2 and its use in understanding the climate effects of increased greenhouse gas concentrations. Weather 62, 307–311.

Hansen, J., Ruedy, R., Sato, M., Lo, K., 2010. Global surface temperature change. Rev. Geophys. 48, RG4004. http://dx.doi.org/10.1029/2010RG000345.

Hansen, J., Sato, M., Ruedy, R., 2012. PNAS plus: perception of climate change. Proc. Natl. Acad. Sci. 109, E2415–E2423. http://dx.doi.org/10.1073/pnas.1205276109.

Hegerl, G., Zwiers, F., 2011. Use of models in detection and attribution of climate change. Interdiscip. Rev. Clim. Change 2, 570–591. http://dx.doi.org/10.1002/wcc.121.

Hegerl, G.C., Hasselmann, K., Cubasch, U., Mitchell, J.B.F., Roeckner, E., Voss, R., Waszkewitz, J., 1977. Multi-fingerprint detection and attribution analysis of greenhouse gas, greenhouse gas-plus-aerosol and solar forced climate change. Clim. Dyn. 13, 613–634.

Hyndman, R.J., Khandakar, Y., 2008. Automatic time series forecasting: the forecast package for R. J. Stat. Softw. 26 (3).

IPCC, 2007. Climate change 2007: the physical science basis. In: Solomon, S., Qin, D., Manning, M., Chen, Z., Marquis, M., Avery, K.B., Tignor, M., Miller, H.L. (Eds.), Contribution of Working Group I to the Fourth Assessment Report of the Intergovernmental Panel on Climate Change. Cambridge University Press, Cambridge, United Kingdom and New York, NY, USA, p. 996.

IPCC, 2013. Climate change 2013: the physical science basis. In: Stocker, T.F., Qin, D., Plattner, G.-K., Tignor, M., Allen, S.K., Boschung, J., Nauels, A., Xia, Y., Bex, V., Midgley, P.M. (Eds.), Contribution of Working Group I to the Fifth Assessment Report of the Intergovern mental Panel on Climate Change. Cambridge University Press, Cambridge, United Kingdom and New York, NY, USA, p. 1535.

Leiserowitz, A., Maibach, E., Roser-Renouf, C., Smith, N., 2011. Climate change in the American Mind: Americans' global warming beliefs and attitudes in May 2011. Yale University and George Mason University. New Haven, CT: Yale Project on Climate Change Communication. Available from: <http://environment.yale.edu/climate/files/ClimateBeliefsMay2011.pdf>.

Ljung, G.M., Box, G.E.P., 1978. On a measure of lack of fit in time series models. Biometrika 65, 297–303.

Maddala, G.S., 2001. Introduction to Econometrics. Wiley, Ontario.

Medvigy, D., Beaulieu, C., 2012. Trends in daily solar radiation and precipitation coefficients of variation since 1984. J. Clim. 25, 1330–1339. http://dx.doi.org/10.1175/2011JCLI4115.1.

Meinshausen, M., Smith, S.J., Calvin, K.V., Daniel, J.S., Kainuma, M., Lamarque, J.-F., Matsumoto, K., Montzka, S.A., Raper, S.C.B., Riahi, K., Thomson, A.M., van Velders, G.J.M., Vuuren, D., 2011. The RCP greenhouse gas concentrations and their extension from 1765 to 2300. Clim. Change 109, 213–241. http://dx.doi.org/10.1007/s10584-011-0156-z (Special Issue).

Myhre, G., Highwood, E.J., Shine, K.P., Stordal, F., 1998. New estimates of radiative forcing due to well mixed greenhouse gases. Geophys. Res. Lett. 25, 2715–2718.

NOAA National Climate Data Centre, 2011. State of the Climate: Global Analysis for May 2011. Available from: <http://www.ncdc.noaa.gov/sotc/global/2011/5>.

Osgood, D.E., Hellmuth, M.E., 2009. Index insurance and climate risk: Prospects for development and disaster management. In: Annex to Hellmuth, M.E., Osgood, D.E., Hess, U., Moorhead, A., Bhojwani, H. (eds), Climate and Society No. 2. International Research Institute for Climate and Society (IRI), Columbia University, New York, USA.

Plimer, I., 2009. Heaven and Earth: Global Warming – The Missing Science. Connor Court Publishing, Ballan, Victoria.

Power, S.B., Smith, I.N., 2007. Weakening of the Walker Circulation and apparent dominance of El Niño both reach record levels, but has ENSO really changed? Geophys. Res. Lett. 37, 1–4.

Rhamstorf, S., Coumou, D., 2011. Increase of extreme events in a warming world. Proc. Natl. Acad. Sci. 108, 17905–17909.

Royston, P., 1982. An extension of Shapiro and Wilk's W test for normality to large samples. Appl. Stat. 31, 115–124.

Shumway, R.H., Stoffer, D.S., 2011. Time Series Analysis and Its Applications. With R Examples, third ed. Springer, New York.

Smith, T.M., Reynolds, R.W., Peterson, T.C., Lawrimore, J., 2008. Improvements to NOAA's historical merged land-ocean surface temperature analysis (1880–2006). J. Clim. 21, 2283–2296.

Tett, S.F.B., Stott, P.A., Allen, M.R., Ingram, W.J., Mitchell, J.F.B., 1999. Causes of twentieth-century temperature change near the Earth's surface. Nature 339, 569–572.

Wang, Y.-M., Lean, J.L., Sheeley Jr., N.R., 2005. Modeling the sun's magnetic field and irradiance since 1713. Astrophys. J. 625, 522–538.